Transient terahertz conductivity in photoexcited silicon nanocrystal films

D. G. Cooke,[1] A. N. MacDonald,[1] A. Hryciw,[1] J. Wang,[2] Q. Li,[2] A. Meldrum,[1] and F. A. Hegmann[1,*]
[1]*Department of Physics, University of Alberta, Edmonton, Alberta, Canada T6G 2J1*
[2]*Department of Physics, The Chinese University of Hong Kong, Shatin, NT, Hong Kong*
(Received 24 March 2006; published 19 May 2006)

Time-resolved terahertz spectroscopy is used to probe ultrafast carrier dynamics and terahertz conductivity in photoexcited thin films of silicon nanocrystals, polynanocrystalline silicon, and epitaxial silicon-on-sapphire. We show that a Drude-Smith model provides an excellent fit to the observed transient terahertz conductivity in all of our samples, revealing a transition from a Drude-like response with low carrier backscatter in bulk silicon-on-sapphire to a non-Drude-like, localized behavior with high carrier backscatter in the silicon nanocrystal films. Evidence for long-range conduction between nanocrystals is observed, and we show that the photoconductive lifetime of the silicon nanocrystals is dominated by trapping at Si/SiO_2 interface states.

DOI: 10.1103/PhysRevB.73.193311 PACS number(s): 78.67.Bf, 72.60.+g, 78.47.+p

Silicon nanocrystals (Si-NCs) have been extensively studied over the past decade, motivated primarily by the possibility of integrating their tunable luminescent properties into future photonic devices.[1,2] Despite this intense research effort, relatively few studies have explored carrier dynamics in silicon nanocrystals on picosecond time scales immediately following optical injection.[3–5] The behavior of charge carriers in semiconductor nanocrystal thin films depends strongly on the structural details. Characteristic length scales such as the crystal size and interparticle spacing determine the transport properties. Transport over macroscopic length scales is dependent on percolation paths spanning the sample dimensions. These may occur provided the nanocrystals are in electrical contact, or if there is a possibility of hopping or tunneling between localized states due to their proximity to one another. Steady-state (low-frequency) conductivity measurements probe this macroscopic connectivity, and recent temperature and field-dependent studies have reported variable range hopping to be important in doped CdSe nanoparticle arrays.[6]

High-frequency measurements, however, can probe conductivity over shorter length scales given by $L_\omega=\sqrt{D/\omega}$, where D is the diffusion coefficient and ω is the probing frequency.[7] Heuristically, this can be thought of as the distance a carrier diffuses before the field reverses direction. In the nanometer length-scale range ($L_\omega=2-10$ nm) and for typical diffusion coefficients ($D\cong 1$ cm^2/s), the corresponding frequency is in the terahertz (THz) region (0.2–4 THz). Thus, by examining the response of an electromagnetic field in the THz frequency range, one can directly observe the influence of nm-scale disorder on carrier motion. Time-resolved THz spectroscopy (TRTS) is a relatively new ultrafast technique that allows transient carrier dynamics and terahertz conductivity to be measured in photoexcited materials over picosecond time scales.[8–18] Whereas Drude-like behavior is typically seen for the THz conductivity of photoexcited carriers in bulk single-crystal samples,[15–17] non-Drude behavior and carrier localization resulting in a suppression of the real conductivity at lower frequencies have been reported in InP and TiO_2 nanocrystals,[13,14] which was shown to be consistent with a generalized Drude formula developed by Smith [19] (referred to here as the "Drude-Smith" model). In another study of ion-implanted Si-NCs (3–4 nm) in SiO_2, the THz conductivity of the photoexcited carriers was modeled as Lorentz oscillators in a background dielectric.[4] However, no dynamics were reported, the nanocluster size dependence or separation was not explored, and the signal-to-noise ratio was limited by low pump powers from the laser source. More recently, a plasmon resonance model (similar to the Lorentz model) was used to describe the THz conductivity in photoexcited micron-sized silicon particles embedded in a polymer matrix.[20]

In this Brief Report, we report both the ultrafast dynamics and frequency-dependent complex THz conductivity of photoexcited silicon films with varying degrees of structural disorder ranging from bulk-Si to Si-NCs in glass. We observe a clear transition in the transient THz conductivity from a Drude-like, free-carrier response in bulk Si to non-Drude, localized behavior in the Si-NC samples, and we find that this transition from free to localized behavior can be described quite well within the framework of the Drude-Smith model. In particular, the real component of the THz conductivity for the Si-NCs is suppressed at low frequencies due to carrier localization, but is nonzero as $\omega\rightarrow 0$ (dc), indicative of long-range transport between nanocrystals. Finally, we find that the ultrafast carrier relaxation dynamics for times greater than 1 ps is dominated by Si/SiO_2 interface trap states and depends on the size of the nanoclusters.

The Si-NC samples were formed by annealing of SiO_x films with $x=1$. This system offers easily tunable crystallite size and density simply by changing the anneal temperature.[2,21–23] For this work, a 1 μm thick SiO film was deposited by thermal evaporation on a 1 mm thick fused silica substrate. The wafer was then divided and annealed for 1 h under $\sim$1 atm of $5\%H_2+95\%N_2$ at anneal temperatures (T_a) from 500–1100 °C. Annealing results in a phase segregation process according to the equation $2SiO\leftrightarrow Si+SiO_2$, producing densely packed Si nanoclusters embedded in an insulating SiO_2 matrix.[21,22] The size and crystallinity of these particles are dependent on T_a, with evidence of amorphous clusters present at lower T_a in the range from 500 to 800 °C and crystalline clusters for $T_a>900$ °C.[22,23] We have veri-

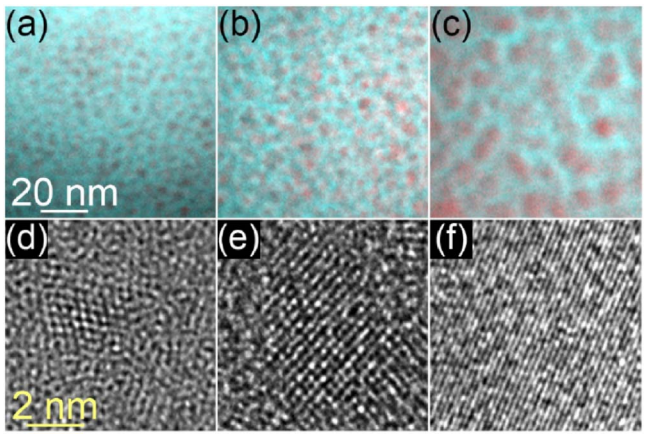

FIG. 1. (Color online) EFTEM (red=Si, blue=O) (a)–(c) and HRTEM (d)–(f) images of the T_a=900 °C (a), (d), 1000 °C (b), (e), and 1100 °C (c), (f) silicon nanocrystal samples.

fied this phase segregation process with energy filtered transmission electron microscopy (EFTEM), as shown in Figs. 1(a)–1(c), and high-resolution TEM (HRTEM), as seen in Figs. 1(d)–1(f), for T_a=900, 1000, and 1100 °C. A ripening process occurs with increasing T_a, showing nanocrystals with diameters of ~3 nm at 900 °C, ~4 nm at 1000 °C, and ~7 nm at 1100 °C. Assuming 100% phase segregation, nanoparticle densities are estimated as 21.0, 9.1, and 1.7($\times 10^{18}$) cm^{-3} for the T_a=900, 1000, and 1100 °C films, respectively. This gives an interparticle (surface-to-surface) spacing that increases with T_a of 0.7, 0.9, and 1.4 nm for the T_a=900, 1000, and 1100 °C films, respectively. A 200 nm thick Si film was also grown on a 1.0 mm thick fused silica substrate by *e*-beam evaporation and annealed under the same conditions at 900 °C, forming a polynanocrystalline silicon (poly-nc-Si) film with 15–25 nm domain sizes. Finally, a bulklike, 200 nm thick epitaxial silicon film on a $(1\bar{1}02)$ sapphire substrate (silicon-on-sapphire, or SOS) was also studied for comparison to the nanocrystalline silicon samples.

The experimental setup has been described elsewhere.[10,11] Briefly, 800 nm, 100 fs laser pulses from a 1 kHz Ti:sapphire laser source are used to generate THz pulses by optical rectification in a ZnTe crystal, and the electric field of the THz pulses are detected by free-space electro-optic sampling in a second ZnTe crystal. Samples were mounted on 1.5 mm diameter apertures at the focus of the THz probe beam and photoexcited with 400 nm pump pulses at room temperature. The electric field of the THz pulse waveform, $E(t)$, transmitted through the sample was measured for a given probe time delay, Δt, with respect to the 400 nm pump pulse. A reference THz pulse, $E_{\mathrm{ref}}(t)$, is also taken at large negative probe time delays ($\Delta t \ll 0$) through the unexcited sample. The Fourier transforms of these THz waveforms, $\Delta E(\omega)$ and $E_{\mathrm{ref}}(\omega)$, can then be used to extract the frequency-dependent complex conductivity $\tilde{\sigma}(\omega)=\sigma_1(\omega)+i\sigma_2(\omega)$ of the photoexcited samples at THz frequencies.[4,8,11–18,20]

In order to probe the relaxation dynamics of the transient photoconductivity induced in the samples, the negative differential transmission of the main peak of the THz pulse,

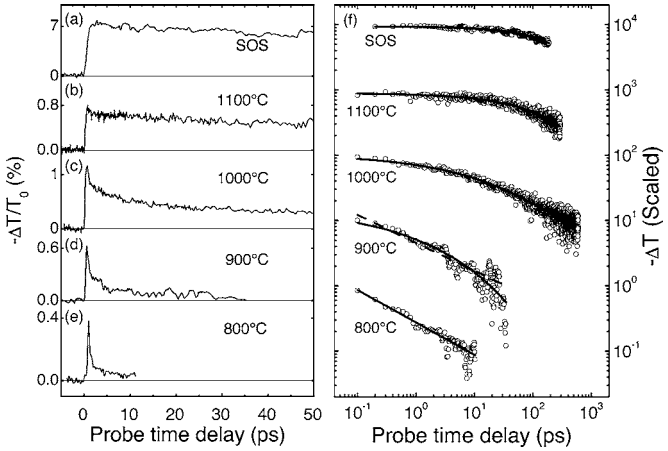

FIG. 2. Differential THz transmission dynamics, $-\Delta T/T_0$, due to 400 nm excitation for (a) an epitaxial silicon-on-sapphire (SOS) film at a pump fluence of F=30 μJ/cm^2, and (b)–(e) Si-NC films (T_a=1100–800 °C) at a pump fluence of F=315 μJ/cm^2. (f) Corresponding log-log plots of the differential THz signals shown in (a)–(e) but over longer time scales and scaled for clarity. The solid lines are fits to the decay dynamics: biexponential for SOS, stretched exponential for Si-NCs with T_a=900, 1000, and 1100 °C, and power law for Si-NCs with T_a=800 and 900 °C (dashed). Fit parameters are given in the text.

$-\Delta T/T_0$, was monitored as a function of THz probe delay time, Δt, with respect to the pump pulse, where T_0 is the amplitude of the reference THz pulse transmitted through the unexcited sample.[8–18] This provides information on the excitation and decay dynamics with a temporal resolution of about 0.5 ps. Figure 2 shows the negative differential transmission ($-\Delta T/T_0$) of the THz probe pulse in the Si-NC films annealed from 800–1100 °C and the SOS sample. A significant increase in the photoconductive lifetime is observed with increasing anneal temperature in the Si-NC samples, ranging from a resolution-limited response for $T_a<700$ °C (not shown) to a few hundred ps at 1100 °C, which is still shorter than the decay time seen in the bulklike SOS film. We see a transition from a power-law decay of $\Delta t^{-\alpha}$ with $\alpha=0.48\pm0.02$ for the T_a=800 °C Si-NC sample to a stretched exponential decay at anneal temperatures of 1000 and 1100 °C of the form $-\Delta T/T_0 \propto \exp[-(\Delta t/\tau_K)^{\beta}]$ with a small constant offset, which is always less than 5% of the peak value. The fitting parameters are τ_K =9.2±0.7 ps(217±6 ps) and $\beta=0.35\pm0.01(0.53\pm0.02)$ for the 1000 °C(1100 °C) films. For the 900 °C Si-NC film, a small signal-to-noise ratio prohibits definitive analysis of the decay dynamics, and so both forms are shown in Fig. 2(f) for comparison. It is likely that the change in dynamics from power law to stretched exponential at this anneal temperature is related to the amorphous-to-crystalline transition observed in the Si-NC samples for $T_a>900$ °C, as discussed earlier. A stretched exponential decay can arise from a distribution of relaxation times and has been observed in time-resolved photoluminescence (PL) studies of Si-NCs over microsecond time scales,[24] including our own samples.

The relaxation dynamics were independent of excitation density (pump fluence). This rules out nonlinear recombina-

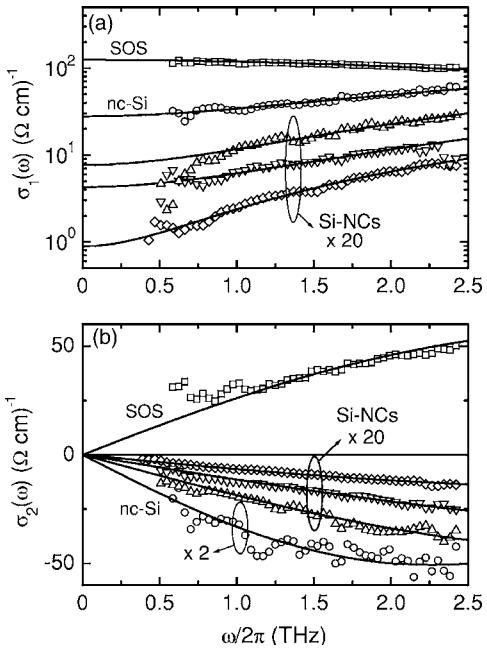

FIG. 3. Terahertz conductivity spectra showing (a) $\sigma_1(\omega)$ and (b) $\sigma_2(\omega)$ for the SOS film (□) 100 ps after excitation (30 μJ/cm^2), poly-nc-Si film (○) 10 ps after excitation (110 μJ/cm^2), and Si-NC films annealed at 900 °C (△), 1000 °C (▽), and 1100 °C (◇) at probe time delays of 4, 10, and 100 ps, respectively (550 μJ/cm^2). Solid lines are fits to the Drude-Smith model with parameters given in Table I.

tion processes like Auger recombination, consistent with transient absorption studies by Klimov *et al.*,[3] which concluded that the fast relaxation dynamics was due to trapping at Si/SiO_2 interface states within 10 ps, consistent with the relaxation dynamics reported here. To determine the role of interface states in our Si-NC films, we compared the transient response of two identical Si-NC films, both annealed at 1000 °C for 1 h, but one annealed in N_2+H_2 and the other only in N_2. When H_2 is included in the annealing process, it is known that it diffuses into the film and passivates dangling bonds (so-called "P_b" centers) at the NC surfaces.[25,26] This effectively depletes a nonradiative recombination channel and results in an increased PL efficiency at ~900 nm by a factor of ~15 in our specimen. The film annealed without H_2 also showed a stretched exponential decay with $\tau_K = 2.9 \pm 0.4$ ps, ~3 times faster than the surface-passivated sample. The lower PL efficiency and the shorter carrier lifetime in the sample not annealed in H_2 are consistent with rapid carrier capture at Si/SiO_2 interface states. This is further supported by the transient signals in smaller nanoclusters (formed at lower T_a) decaying much faster due to a higher surface-area-to-volume ratio, also in agreement with previous work.[3]

Figure 3 shows the complex conductivity spectra for epitaxial SOS, poly-nc-Si, and three Si-NC samples ($T_a = 900, 1000, 1100$ °C). The complex conductivity of the bulklike SOS sample is well described by a simple Drude model with a plasma frequency $\omega_P/2\pi = 32 \pm 1$ THz($\omega_P^2 = ne^2/\varepsilon_0 m^*$) and a scattering time $\tau = 35 \pm 1$ fs, as shown by the fits (solid lines) to both the real and imaginary components of the conductivity. Assuming an electron effective mass $m^* = 0.26 m_e$,[27] these fit parameters correspond to a carrier density $n = 3.3 \times 10^{18}$ cm^{-3} and a carrier mobility $\mu = e\tau/m^* = 240$ cm^2/Vs, in reasonable agreement with an estimate of $n_{max} = 3.1 \times 10^{18}$ cm^{-3} from the experimental pump fluence and an optical penetration depth of $\delta_{400\ nm} = 82$ nm (Ref. 28) and literature values for the carrier mobility in SOS of $\mu = 200-400$ cm^2/Vs.[29] Examining the poly-nc-Si and Si-NC spectra in Fig. 3, two features are evident. The first is a shift of spectral weight in $\sigma_1(\omega)$ away from zero frequency, which becomes more pronounced in the Si-NC films, and a negative $\sigma_2(\omega)$. These features are incompatible with a Drude model or its simple derivatives,[15,27] and have been observed in systems exhibiting localization of charge carriers.[4,13,14,18,30]

TABLE I. Parameters for the Drude-Smith fits in Fig. 3.

Sample	τ (fs)	c	μ_m (cm^2/V s)
SOS	35±1	−0.007±0.004	240±7
Poly-nc-Si	26±1	−0.830±0.010	30±3
Si-NC(900 °C)	16±1	−0.962±0.002	4.2±0.2
Si-NC(1000 °C)	12.9±0.5	−0.972±0.002	2.4±0.3
Si-NC(1100 °C)	17.6±0.5	−0.983±0.001	1.7±0.2

The Drude-Smith model[19] is a relatively simple classical model that was formulated to describe systems in which the real part of the conductivity is suppressed by disorder by incorporating memory effects in the scattering process. The complex conductivity in the Drude-Smith formalism is given by[19]

$$\tilde{\sigma}(\omega) = \frac{ne^2\tau/m^*}{1 - i\omega\tau}\left[1 + \sum_{j=1} \frac{c_j}{(1 - i\omega\tau)^j}\right], \qquad (1)$$

where c_j is a parameter describing the persistence of velocity after some number j of scattering events. In practice, it is easier to take only the first term in the summation in Eq. (1) such that $c_1 = c$ and $c_j = 0$ for $j > 1$. In this case, c can vary between 0 and −1, corresponding to Drude conductivity for $c = 0$ and complete carrier backscattering, or localization, for $c = -1$. This model has been successfully applied to the transient THz conductivity observed in InP and TiO_2 nanocrystals,[13,14] but has been criticized as being unphysical, citing that it requires carriers to scatter only once.[20] However, this need not be true since, as was suggested by Smith,[19] the set of c_j for $j > 1$ can all be zero, corresponding to a transition from ballistic to diffusive propagation where the persistence of velocity occurs only for the first scattering event.

Excellent fits to the Drude-Smith model in Eq. (1) with $c_j = 0$ for $j > 1$ are obtained *simultaneously* for *both* $\sigma_1(\omega)$ and $\sigma_2(\omega)$, as shown in Fig. 3, for a given set of fit parameters ω_p, τ, and c, as summarized in Table I. A fit to the 1100 °C Si-NC data using a Drude-Lorentz model required an oscillator with a center frequency of about 9 THz (~37 meV) with an unphysically small oscillator damping time of 10 fs (~70 meV). Many other models, including ef-

fective medium theory,[4] various two-site hopping models,[31] plasmon resonances,[20] and localized-Drude models[30] were also considered; however, the Drude-Smith model provided a superior fit to both σ_1 and σ_2 for *all* the samples investigated from bulk SOS to poly-nc-Si and Si-NCs. The power of the Drude-Smith model is in its ability to describe the transition in the observed THz conductivity from a free-carrier, Drude-like response to localized behavior with essentially a single parameter c corresponding to the persistence of velocity or amount of carrier backscatter.[19]

Long-range transport, which is hindered by disorder, is also parametrized by c in the Drude-Smith model. The macroscopic dc mobility in the Drude-Smith model is given by $\mu_m=\mu(1+c)$, where μ is the carrier mobility in the bulk single-crystal phase. The real component of the THz conductivity for the poly-nc-Si sample in Fig. 3(a) shows a dc conductivity which is suppressed ($c=-0.83\pm0.01$) but certainly not zero. This reflects the partial carrier localization within the nanocrystalline Si grains with long-range transport between the connected grains. The real conductivity for the Si-NC samples in Fig. 3(a) shows a dc conductivity that is highly suppressed with c as high as -0.983 ± 0.001 for the sample annealed at 1100 °C. Here, injected carriers are primarily localized to their parent nanocrystals where they remain highly mobile on nanometer-length scales, but their macroscopic mobility is greatly diminished due to the insulating SiO_2 barriers between the nanocrystals hindering long-range motion. That the dc conductivity is not extinguished entirely suggests tunneling or hopping between the silicon nanocrystals. This is further supported by examining how μ_m varies with anneal temperature, as listed in Table I. With increasing T_a, the Si-NC particle density decreases so that the spacing between nanocrystals increases. It is then reasonable to expect that hopping or tunneling between nanocrystals would be suppressed in samples annealed at higher temperatures, resulting in the observed lowering of the macroscopic mobility μ_m at higher anneals. To test for the existence of a macroscopic dc mobility for photoinjected carriers in the Si-NC films, we performed a steady-state photoconductivity experiment on the 1000 °C Si-NC sample by depositing an interdigitated Cr/Au electrode structure (10 μm finger width and spacing) on top of the Si-NC film and illuminating the active region with a HeCd laser at a wavelength of 442 nm. The resistance was greater than 300 GΩ in the dark state and about 10 GΩ when illuminated with the laser source, proving the existence of a macroscopic dc photoconductivity in the Si-NC samples consistent with the THz conductivity results as $\omega\rightarrow0$.

In summary, we have investigated the transient THz conductivity of silicon thin films with various degrees of structural disorder. A Drude-Smith model was used to describe a transition in the THz conductivity from Drude-like in bulk-Si to more localized behavior in poly-nc-Si and Si-NCs in SiO_2. The lifetime of the transient photoconductivity in the Si-NC films was found to be dominated by trapping at interface states, decaying on a 1–200 ps time scale depending on the anneal temperature. Evidence for long-range transport in the Si-NC samples was also observed.

The authors thank J. Gao for the Cr/Au electrode deposition and acknowledge helpful discussions with F. Marsiglio and A. Slepkov, and financial support from NSERC, CIPI, and iCORE.

*Electronic address: hegmann@phys.ualberta.ca

[1] L. Pavesi *et al.*, Nature (London) **408**, 440 (2000).
[2] A. Hryciw *et al.*, Adv. Mater. (Weinheim, Ger.) **17**, 845 (2005); A. N. MacDonald *et al.*, Opt. Mater. **28**, 820 (2006).
[3] V. I. Klimov *et al.*, Appl. Phys. Lett. **73**, 2603 (1998).
[4] H. Altan *et al.*, J. Appl. Phys. **96**, 6685 (2004).
[5] F. Trojánek *et al.*, Phys. Rev. B **72**, 075365 (2005).
[6] D. Yu *et al.*, Phys. Rev. Lett. **92**, 216802 (2004).
[7] P. F. Henning *et al.*, Phys. Rev. Lett. **83**, 4880 (1999).
[8] C. A. Schmuttenmaer, Chem. Rev. (Washington, D.C.) **104**, 1759 (2004).
[9] P. Uhd Jepsen *et al.*, Appl. Phys. Lett. **79**, 1291 (2001).
[10] D. G. Cooke *et al.*, Appl. Phys. Lett. **85**, 3839 (2004).
[11] O. Ostroverkhova *et al.*, Phys. Rev. B **71**, 035204 (2005).
[12] R. P. Prasankumar *et al.*, Appl. Phys. Lett. **86**, 201107 (2005).
[13] M. C. Beard *et al.*, Nano Lett. **3**, 1695 (2003).
[14] G. M. Turner *et al.*, J. Phys. Chem. B **106**, 11716 (2002).
[15] M. C. Beard *et al.*, Phys. Rev. B **62**, 15764 (2000).
[16] J. Shan *et al.*, Phys. Rev. Lett. **90**, 247401 (2003).
[17] R. A. Kaindl *et al.*, Nature (London) **423**, 734 (2003).
[18] E. Hendry *et al.*, Phys. Rev. B **71**, 125201 (2005).
[19] N. V. Smith, Phys. Rev. B **64**, 155106 (2001).
[20] H. K. Nienhuys and V. Sundström, Appl. Phys. Lett. **87**, 012101 (2005).
[21] K. Furukawa *et al.*, Appl. Phys. Lett. **72**, 725 (1998).
[22] L. X. Yi *et al.*, J. Phys.: Condens. Matter **15**, S2887 (2003).
[23] A. Meldrum *et al.*, J. Vac. Sci. Technol. A **24**, 713 (2006).
[24] R. Chen, J. Lumin. **102**, 510 (2003).
[25] S. P. Withrow *et al.*, J. Appl. Phys. **86**, 396 (1999).
[26] D. Comedi *et al.*, Appl. Phys. Lett. **87**, 213110 (2005).
[27] T.-I. Jeon and D. Grischkowsky, Phys. Rev. Lett. **78**, 1106 (1997).
[28] E. D. Palik, *Handbook of Optical Constants of Solids* (Academic, London, 1998).
[29] D. McLeod Jr. *et al.*, J. Vac. Sci. Technol. A **7**, 1322 (1989).
[30] T.-I. Jeon *et al.*, Synth. Met. **135**, 451 (2003).
[31] J. A. Reedijk *et al.*, Phys. Rev. B **57**, R15116 (1998).